Canonical transient receptor potential 6 channel deficiency promotes smooth muscle cells dedifferentiation and increased proliferation after arterial injury

Andrew H. Smith, MD,[a,b] Priya Putta, PhD,[b] Erin C. Driscoll, BS,[b] Pinaki Chaudhuri, PhD,[b] Lutz Birnbaumer, PhD,[c,d] Michael A. Rosenbaum, MD,[b,e] *and* Linda M. Graham, MD,[a,b] *Cleveland, Ohio; Research Triangle Park, NC; and Buenos Aires, Argentina*

ABSTRACT

Objective: Previous studies showed the benefit of canonical transient receptor potential 6 (TRPC6) channel deficiency in promoting endothelial healing of arterial injuries in hypercholesterolemic animals. Long-term studies utilizing a carotid wire-injury model were undertaken in wild-type (WT) and TRPC6$^{-/-}$ mice to determine the effects of TRPC6 on phenotypic modulation of vascular smooth muscle cells (SMC) and neointimal hyperplasia. We hypothesized that TRPC6 was essential in the maintenance or reexpression of a differentiated SMC phenotype and minimized luminal stenosis following arterial injury.

Methods: The common carotid arteries (CCA) of WT and TRPC6$^{-/-}$ mice were evaluated at baseline and 4 weeks after wire injury. At baseline, CCA of TRPC6$^{-/-}$ mice had reduced staining of MYH11 and SM22, fewer elastin lamina, luminal dilation, and wall thinning. After carotid wire injury, TRPC6$^{-/-}$ mice developed significantly more pronounced luminal stenosis compared with WT mice. Injured TRPC6$^{-/-}$ CCA demonstrated increased medial/intimal cell number and active cell proliferation when compared with WT CCA. Immunohistochemistry suggested that expression of contractile biomarkers in medial SMC were essentially at baseline levels in WT CCA at 28 days after wire injury. By contrast, at 28 days after injury medial SMC from TRPC6$^{-/-}$ CCA showed a significant decrease in the expression of contractile biomarkers relative to baseline levels. To assess the role of TRPC6 in systemic arterial SMC phenotype modulation, SMC were harvested from thoracic aortae of WT and TRPC6$^{-/-}$ mice and were characterized. TRPC6$^{-/-}$ SMC showed enhanced proliferation and migration in response to serum stimulation. Expression of contractile phenotype biomarkers, MYH11 and SM22, was attenuated in TRPC6$^{-/-}$ SMC. siRNA-mediated TRPC6 deficiency inhibited contractile biomarker expression in a mouse SMC line.

Conclusions: These results suggest that TRPC6 contributes to the restoration or maintenance of arterial SMC contractile phenotype following injury. Understanding the role of TRPC6 in phenotypic modulation may lead to mechanism-based therapies for attenuation of IH. (JVS—Vascular Science 2020;1:136-50.)

Clinical Relevance: After endovascular intervention and open vascular surgery, vascular smooth muscle cells (VSMC) undergo a coordinated reprogramming of gene expression to facilitate arterial healing. Down regulation of VSMC-specific contractile biomarkers (eg, SM22 and MYH11) and induction of pathways that promote cell proliferation, migration, and matrix synthesis are hallmarks of this phenotypic switch. Dysregulated phenotypic switching leads to the development of neointimal hyperplasia and vascular restenosis. Identifying pathways that regulate or constrain VSMC phenotypic modulation, therefore, has the potential to decrease neointimal hyperplasia and improve outcomes after vascular intervention. In this study, we demonstrate that depletion of the non-voltage-gated cation channel TRPC6 promotes phenotypic switching and loss of contractile biomarkers in systemic arterial VSMC. TRPC6$^{-/-}$ mice developed significantly more pronounced luminal stenosis compared with wild-type mice after carotid wire injury. These results suggest that TRPC6 contributes to the restoration or maintenance of contractile phenotype in VSMC after injury. Understanding the role of TRPC6 in phenotypic switching may lead to mechanism-based therapies to mitigate restenosis.

Keywords: Smooth muscle cells; TRPC6; Phenotypic modulation; Intimal hyperplasia; Carotid injury

From the Department of Vascular Surgery,[a] and Department of Biomedical Engineering,[b] Cleveland Clinic, Cleveland; the Neurobiology Laboratory, National Institute of Environmental Health Sciences, Research Triangle Park[c]; the Institute of Biomedical Research (BIOMED), Catholic University of Argentina, Buenos Aires[d]; and the Surgical Service, Louis Stokes Cleveland Veterans Affairs Medical Center, Cleveland.[e]

Supported by Grant Number HL064357 from the National Heart, Lung, and Blood Institute. The content is solely the responsibility of the authors and does not necessarily represent the official views of the National Heart, Lung, and Blood Institute or the National Institutes of Health. Supported in part by The Intramural Research Program of the NIH (Project Z01-ES-101684 to LB); and by Career Development Award #IK2BX003628 from the United States (U.S.) Department of Veterans Affairs Biomedical Laboratory Research and Development Service. The contents do not represent the views of the U.S. Department of Veterans Affairs or the United States Government.

Author conflict of interest: none.

Correspondence: Linda M. Graham, MD, Department of Biomedical Engineering ND20, Cleveland Clinic, 9500 Euclid Ave, Cleveland, OH 44195 (e-mail: grahaml@ccf.org).

The editors and reviewers of this article have no relevant financial relationships to disclose per the JVS-Vascular Science policy that requires reviewers to decline review of any manuscript for which they may have a conflict of interest.

2666-3503

https://doi.org/10.1016/j.jvssci.2020.07.002

Treatment of coronary and peripheral vascular disease often requires angioplasty with or without stenting or placement of vascular grafts. The long-term results of all vascular interventions are compromised by delayed endothelial cell (EC) healing with continued thrombogenicity of the luminal surface and by the development of neointimal hyperplasia (IH). More rapid reendothelialization limits IH,[1-3] which is driven, in part, by phenotypic modulation of vascular smooth muscle cells (VSMC).[4] Under basal conditions, medial VSMC control systemic vasomotor tone through regulated expression and activation of calcium permeable ion channels and VSMC-specific contractile proteins.[5,6] After arterial injury, VSMC dedifferentiate into clonally proliferative, prosynthetic progenitors that expand in the subendothelial compartment and can form hyperplastic lesions.[4,6] Decreased VSMC contractile gene expression programs, and upregulation of pathways that facilitate proliferation and migration into the subendothelial space are hallmarks of this phenotypic switch.[7]

Regulated expression of calcium-permeable ion channels is essential to maintain functional properties of both contractile and phenotypically modulated VSMC.[5,8] Canonical transient receptor potential 6 (TRPC6) channels are highly expressed in human arterial vascular tissue and within both EC and SMC. TRPC6 forms homo- and heterotetrameric nonselective cation channels with TRPC3 and 7 to mediate receptor and store operated calcium entry.[9,10] TRPC6 is activated by lipid oxidation products and a high cholesterol diet dramatically impairs endothelial healing of carotid injuries in WT mice, but has no effect in *TRPC6*$^{-/-}$ mice.[11,12]

To determine if the benefit of TRPC6 deficiency on EC healing decreased intimal hyperplasia formation, long-term studies were undertaken using wild-type (WT) and TRPC6-deficient mice. Initial common carotid artery (CCA) wire injury studies showed increased SMC mass at 28 days in TRPC6-deficient mice compared with WT mice, suggesting the hypothesis that TRPC6 was essential in the maintenance or re-expression of a differentiated SMC phenotype. Studies of SMC harvested from WT and TRPC6-deficient mice showed that TRPC6 deficiency was associated with increased proliferation and migration in response to serum stimulation. TRPC6 downregulation or deficiency also was accompanied by loss of contractile biomarkers.

ARTICLE HIGHLIGHTS

- **Type of Research:** Experimental basic science research
- **Key Findings:** compared with wild-type mice, canonical transient receptor potential 6 deficient (TRPC6$^{-/-}$) mice show abnormal carotid architecture and develop severe luminal stenosis following carotid wire injury. In cultured smooth muscle cells, TRPC6 depletion decreases expression of contractile biomarkers SM22 and MYH11 and is associated with the emergence of a proliferative phenotype.
- **Take Home Message:** TRPC6 contributes to the restoration or maintenance of arterial smooth muscle cell contractile phenotype and may protect against restenosis after injury.

METHODS

Animal use. WT and *TRPC6*$^{-/-}$ mice on a 1:1 129Sv:C57BL/6J background, as previously described,[13] were used for these studies. Mice were maintained on standard chow diets. *TRPC6* deletion was confirmed by polymerase chain reaction (PCR) using DNA extracted from toe biopsies. The Institutional Animal Care and Use Committee approved the animal use and study protocols. The animal protocols and care complied with the Guide for the Care and Use of Laboratory Animals.

Carotid histology. Mice were anesthetized by intraperitoneal injection of ketamine (80 mg/kg) and xylazine (5 mg/kg). The vasculature was perfusion-fixed with 10 mL phosphate-buffered saline followed by 25 mL 10% neutral-buffered formalin administered through the left ventricle over 30 minutes. Bilateral CCA were mounted in paraffin and sectioned transversely between 1.5 and 2.0 mm proximal to the CCA bifurcation. Sections were incubated with primary antibody for 16 to 24 hours in Tris-buffered saline + 5% bovine serum albumin. Primary antibodies included SM22 (Genetex, Irvine, Calif; cat. GTX101608, 1:100), MYH11 (Santa Cruz Biotechnology, Santa Cruz, Calif; cat. sc-6956, 1:100), α-smooth muscle actin (α-SMA; Cell Signaling Technology, Danvers, Mass; cat. D4K9N, 1:100), and Ki67 (Genetex, cat. GTX16667, 1:100), Von-Willebrand factor (Abcam, Cambridge, UK; cat. ab6994, 1:100). Sections were incubated in secondary antibody for 2 hours in tris-buffered saline + 5% bovine serum albumin and developed with a 3,3'diaminobenzidine (DAB) Substrate Kit (Abcam). For each stain, a minimum of three cross-sections were evaluated per carotid artery. The intensity of medial DAB staining was semiquantitatively assessed using ImageJ software (National Institutes of Health, Bethesda, Md) as previously described.[14] Elastin and collagen were detected by Weitgert's Resorcin Fuchsin (Electron Microscopy Sciences, Hatfield, Pa; Cat. 26370) and Direct Red 80 (Sigma-Aldrich, St Louis, Mo; Cat. 365548) staining respectively according to the manufacturer's protocols. Separately, sections were stained with hematoxylin (Thermo Fisher Scientific, Waltham, Mass; Cat. 7231) and eosin (Thermo Fisher Scientific, Cat. 7111) according to the manufacturer's protocol.

Carotid wire injury. Male mice 10 weeks old were subjected to carotid wire injuries as described by Lindner et al.[15] Briefly, mice were anesthetized by intraperitoneal injection of ketamine (80 mg/kg) and xylazine (5 mg/kg). An 0.014 inch or 0.018 inch wire (Boston Scientific, Marlborough, Mass; V14 or V18 ControlWire Guidewire) was selected for injury based on size of the artery. The wire was passed retrograde three times from the external carotid artery to the CCA origin and the external carotid artery was ligated proximal and distal to the arteriotomy with surgical clips. The left external carotid artery, internal carotid artery, and CCA were dissected from adjacent tissue but not injured. After injury, mice were fed standard chow diets. Bilateral (injured and uninjured) CCA were explanted on day 28 after injury and processed for histology.

Percent CCA dilation was determined as 100 × (wire diameter − uninjured CCA luminal diameter)/uninjured CCA luminal diameter. The percent change in luminal area, medial thickness, or area inside the external elastic lamina was determined as 100 × (injured CCA measurement − uninjured CCA measurement)/uninjured CCA measurement.

Carotid homogenization. After bilateral CCA were dissected free of adjacent tissue, 10 mL of ice-cold phosphate-buffered saline was perfused through the left ventricle. CCA were explanted, immediately placed on ice, and minced. Tissue was resuspended in cell lysis buffer (approximately 300 μL buffer per 5 mg tissue) and incubated at 4°C for 2 to 4 hours. Debris was removed by centrifugation at 12,000 rpm for 10 minutes and the supernatant resolved by sodium dodecyl sulfate polyacrylamide gel electrophoresis (described elsewhere in this article).

VSMC isolation and culture. The thoracic aorta was removed from WT and *TRPC6*$^{-/-}$ mice. Aortic SMC were isolated after collagenase digestion of the aorta as described by Adhikari et al.[16] SMC identity was confirmed by positive staining for SM22 (Genetex, cat. GTX101608) using immunocytochemistry. SMC were cultured in Dulbecco's Modified Eagle Medium (DMEM) and Ham's F-12 (F12) nutrient mixture with 20% fetal bovine serum (FBS) (Hyclone, Logan, Utah; cat. SH30541.03) and 1% penicillin/streptomycin (PS). Cells were grown at 37°C in 5% CO_2 and used in passages one through eight.

Cell proliferation assays. For growth curve analysis, WT and *TRPC6*$^{-/-}$ SMC were seeded into 60 mm diameter plastic culture dishes at a density of 1×10^6 cells/dish. Cells were cultured for 24, 48, 72, or 96 hours. At each time point, cells were trypsinized and counted. The fold change in cell number was determined relative to the 24 hours time point.

In parallel experiments, WT and *TRPC6*$^{-/-}$ SMC were seeded into 24-well culture plates at a density of 3×10^5 cells/well, cultured for 24 hours, and placed in DMEM with 0.25% FBS and 1% PS overnight. Cells were then changed to DMEM with 0.25% FBS alone or DMEM containing 5 ng/mL platelet-derived growth factor-BB (PDGF-BB, Prospec, Rehovet, Israel), 10 ng/mL PDGF-BB, or 10% FBS for 48 hours, trypsinized, and counted. The fold change in cell number was quantified relative to the 0.25% FBS condition.

Cell migration assays. WT and *TRPC6*$^{-/-}$ VSMC were seeded into 12-well culture plates at a density of 2×10^6 cells/well and allowed to adhere overnight. The next day cultures were confluent and made quiescent in DMEM with 0.25% FBS and 1% PS overnight. Cells were then scraped with a 200-μL pipette tip as previously described,[17] washed, and incubated with DMEM with 0.25% FBS, or DMEM containing 5 ng/mL PDGF-BB, 10 ng/mL PDGF-BB, or 10% FBS. Cells were imaged at 0 and 12 hours after scraping using a Luminera INFINITY 1.1M 1.3MP microscope camera and INFINITY CAPTURE software (Ottawa, ON, Canada). The wound area was quantified using ImageJ software and the percent wound closure was calculated.

Immunoblot analysis. Immunoblot analysis was performed after proteins (60-80 μg per lane) were loaded into 4-20% Tris-Gylcine sodium dodecyl sulfate polyacrylamide gel electrophoresis as previously described[18,19] and detected by antibodies specific for TRPC6 (Cell Signaling, cat. D3G1Q, 1:250), TRPC3 (Cell Signaling, cat. D4P5S, 1:250), beta-actin (Cell Signaling, cat. D6A8, 1:10000), SM22 (Genetex, cat. GTX101608, 1:2500), or Myh11 (Genetex, cat. GTX66065, 1:5000).

Quantitative real-time PCR. Total RNA was isolated from cultured WT and *TRPC6*$^{-/-}$ VSMC using the RNAEasy total RNA isolation kit (Qiagen, Hilden, Germany). Messenger RNA (mRNA) (500 ng) was converted to complementary DNA (cDNA) using the iScript cDNA Synthesis Kit (Bio-Rad, Hercules, Calif) using the manufacturer's protocol. Quantitative real-time PCR was performed on the Applied Biosystems (Foster City, Calif) StepOnePlus Real-time PCR system. The Taqman gene expression assays (Thermo Fisher Scientific, cat. 4331182) used included MYH11 (assay no. Mm00443013_m1), SM22 (assay no. Mm0441661_g1), and GAPDH (Mm99999915_g1). GAPDH gene expression served as an endogenous control. The fold difference in expression of target cDNA was determined using the comparative C_T method as previously described.[20]

Small interfering RNA transfection. Immortalized mouse aortic SMC, mouse aortic SMC line (MOVAS) cells (ATCC CRL2797),[21] were grown to 60% to 70% confluency in 6-well culture plates in DMEM/F12 with 10% FBS and 1% PS. Cells were transiently transfected with Lipofectamine 3000 (Thermo Fisher Scientific) and 50 nmol/L

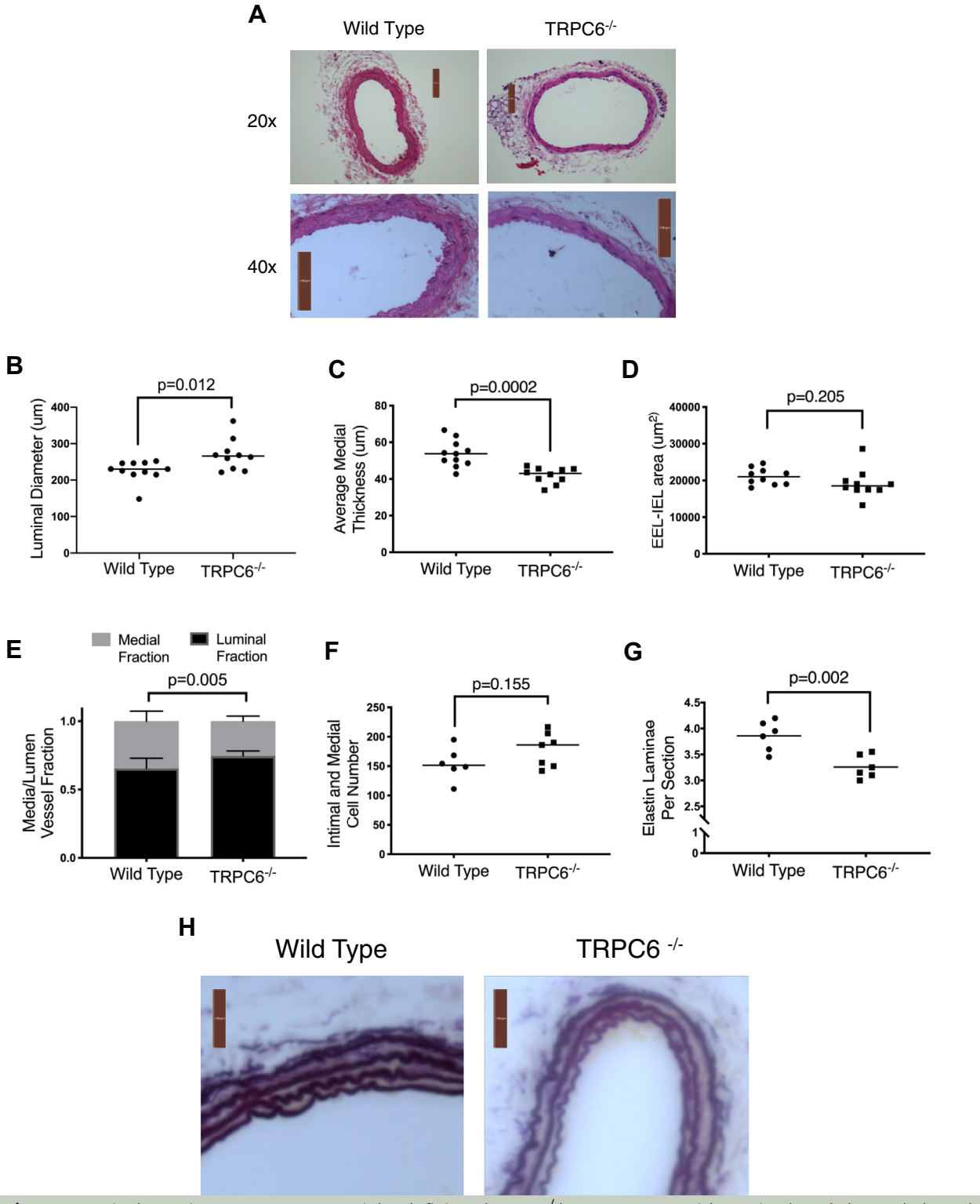

Fig 1. Canonical transient receptor potential 6 deficient (*TRPC6*$^{-/-}$) common carotid arteries (CCA) showed altered basal structure. **A,** Representative cross sections of wild-type (WT) and TRPC6$^{-/-}$ CCA after hematoxylin and eosin staining. (*Top*) WT and TRPC6$^{-/-}$ CCA, at 20× objective. (*Bottom*) WT and TRPC6$^{-/-}$ CCA, at 40× objective. Scale bar height = 100 μm. **B-F,** Measurements of CCA from WT and TRPC6$^{-/-}$ mice (n ≥ 10 mice per genotype, unless specified). **B,** Luminal diameter.**C,** Average medial thickness. **D,** Medial area. **E,** Medial and luminal fraction of total CCA area inside the external elastic lamina (EEL). **F,** Total number of cell nuclei in the media in CCA cross sections from WT and TRPC6$^{-/-}$ mice (n = 6 WT mice, 7 TRPC6$^{-/-}$ mice). **G,** Number of elastic lamellae in the media of CCA cross-sections from WT and TRPC6$^{-/-}$ mice (n = 6 mice per genotype). **H,** Representative CCA cross sections from WT and TRPC6$^{-/-}$ mice stained with Weigert's resorcin-fuchsin stain for elastin fibers. Scale bar height = 100 μm.

scrambled control small interfering RNA (NsiRNA) or siRNA targeting TRPC6 (Dharmacon) for 16 to 24 hours using the manufacturer's protocol. Cells were then transferred into fully supplemented medium for 24 to 32 hours and harvested.

Statistical analysis. In vitro experiments were performed in triplicate with VSMC isolated from at least three different animals. Values were presented as the mean ± standard deviation. Data with two categorical variables were compared using column statistics and the unpaired Student *t*-test. Data with more than two categorical variables were compared using one and two-way analysis of variance with Tukey post hoc test for multiple comparisons. Data were considered statistically significant at an alpha level of a *P* value of less than .05.

RESULTS

Previous studies showed improved endothelial healing of arterial injuries in *TRPC6*$^{-/-}$ mice compared with WT mice in the setting of hypercholesterolemia (eg, mice maintained on high-fat diets).[12] No differences in rates of re-endothelialization were observed in nonhypercholesterolemic WT and TRPC6$^{-/-}$ mice (eg, mice maintained on standard chow diets).[12] SMC proliferation and intimal hyperplasia were not evaluated in these previous studies. The current study was therefore undertaken to determine if improved endothelial healing in hypercholesterolemic TRPC6$^{-/-}$ mice translated to reduced intimal hyperplasia after a wire injury. During the initial phase of these experiments, wire injury was performed on chow-fed, nonhypercholesterolemic WT and TRPC6$^{-/-}$ mice. Unexpectedly, aggressive SMC proliferation was noted in the carotid arteries of injured *TRPC6*$^{-/-}$ mice, but not in the carotid arteries of injured WT mice. Closer inspection by histology revealed alterations in the resting, uninjured arterial structure in *TRPC6*$^{-/-}$ mice. The CCA of *TRPC6*$^{-/-}$ mice had larger luminal diameter and thinner media than WT mice (Fig 1, *A*). On average, *TRPC6*$^{-/-}$ CCA showed a 19.5% increase in luminal diameter ($P = .012$) and a 21.9% decrease in medial thickness (between the internal to external elastic lamina; $P = .0002$) (n ≥ 10 mice per genotype; Fig 1, *B* and *C*). There were no differences in total medial area between WT and *TRPC6*$^{-/-}$ CCA (Fig 1, *D*), although as expected, the luminal area as a fraction of the total vessel area was significantly greater in *TRPC6*$^{-/-}$ CCA (9.1% increase, n ≥ 10 mice per genotype; $P = .005$; Fig 1, *E*). The number of medial cell nuclei was similar between *TRPC6*$^{-/-}$ and WT CCA, suggesting that differences in arterial architecture were not due to abnormal medial investment by VSMC (Fig 1, *F*). The medial elastin content differed by genotype. The number of elastic lamellae was significantly decreased in *TRPC6*$^{-/-}$ CCA cross-sections compared with WT CCA (3.3 ± 0.2 lamellae per *TRPC6*$^{-/-}$ CCA vs 3.9 ± 0.3 lamellae per WT CCA; n = 6 mice per genotype; $P = .002$; Fig 1, *G*; *H*). No difference in medial collagen was detected by Sirius red staining (data not shown). These findings suggested that *TRPC6* gene deficiency subtly alters basal CCA structure.

A murine model of CCA wire injury was used to investigate the role of TRPC6 protein in arterial healing and remodeling. Either a 0.014-inch (0.035 cm) or 0.018-inch (0.045 cm) diameter wire was selected based on carotid artery size. In total, seven WT CCA were injured using a 0.014-inch diameter wire and no WT CCA was injured using a 0.018-inch diameter wire. Four *TRPC6*$^{-/-}$ CCA were injured using 0.014-inch wires and two were injured using 0.018-inch wires. The CCA distention was 30% to 70% over basal diameter in these mice, and the percent CCA dilation was not significantly different between WT and *TRPC6*$^{-/-}$ mice (Fig 2, *A*).

Arterial remodeling in WT and *TRPC6*$^{-/-}$ mice was assessed at 28 days after carotid wire injury. Representative hematoxylin and eosin staining of uninjured and injured WT and TRPC6$^{-/-}$ CCA are shown in Fig 2, *B*. The luminal area was preserved in WT mice (n = 7) after injury, but significantly decreased in TRPC6$^{-/-}$ mice (n = 6) (uninjured vs injured WT: 42,368 ± 5381 vs 35,302 ± 4273; $P = .589$; uninjured vs injured TRPC6$^{-/-}$: 59,870 ± 9020 vs 25,627 ± 18,327; $P < .001$; Fig 2, *C*). The percent change in luminal area after carotid wire injury was greater in *TRPC6*$^{-/-}$ mice (n = 6) than in WT mice (n = 7), −54.98 ± 31.26 vs −15.73 ± 12.73 WT mice, respectively ($P = .011$; Fig 2, *D*). Interestingly, the area contained within the external elastic lamina decreased in *TRPC6*$^{-/-}$ mice, but not in WT mice (−22.93 ± 9.57% in *TRPC6*$^{-/-}$ mice vs 2.57 ± 13.93% in WT mice; $P = .003$; Fig 2, *E*), indicating negative remodeling in *TRPC6*$^{-/-}$ mice. No differences in percent change in medial thickness were observed between genotypes (Fig 2, *F*). Thus, despite similar injuries, *TRPC6*$^{-/-}$ mice developed greater luminal stenosis and more negative remodeling than WT mice.

The effects of carotid injury on cell proliferation and VSMC phenotypic modulation were assessed. At 28 days after injury, cell number was significantly increased in the injured CCA compared with the uninjured CCA in *TRPC6*$^{-/-}$ mice (median cell number per section: 122 in uninjured TRPC6$^{-/-}$ CCA vs 280 in injured TRPC6$^{-/-}$ CCA; n = 6 mice; $P = .015$; Fig 3, *A*). No significant difference in cellularity was observed between the injured and uninjured CCA of WT mice (Fig 3, *A*). Nuclei staining positive for Ki67, a proliferation marker, were observed only in injured *TRPC6*$^{-/-}$ CCA (Fig 3, *B* and *C*). No difference was noted in medial α-SMA staining between uninjured CCA from WT and *TRPC6*$^{-/-}$ mice or between injured and uninjured CCA in WT mice, suggesting that VSMC contractile phenotype had been maintained or had recovered at 28 days after injury in WT mice (Fig 3, *D* and *E*). By contrast, a significant decrease in the staining intensity for α-SMA was observed in the

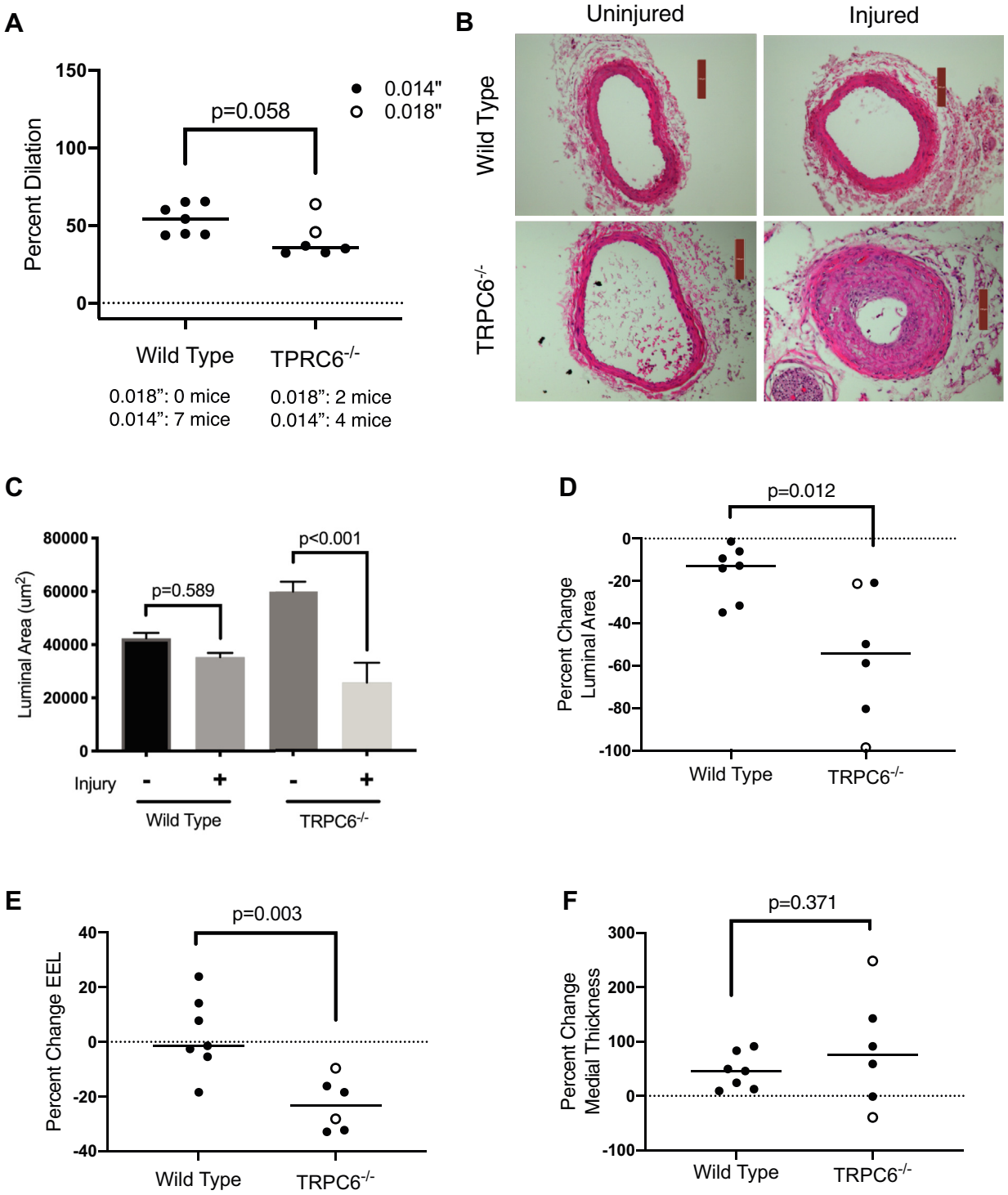

Fig 2. Luminal stenosis and negative remodeling are aggravated in canonical transient receptor potential 6 deficient (*TRPC6*$^{-/-}$) mice after carotid wire injury. **A,** Wild-type (WT) and TRPC6$^{-/-}$ mice were subjected to carotid wire injury using either a 0.014-inch (n = 7 WT and n = 4 TRPC6$^{-/-}$ mice) or 0.018-inch (n = 0 WT and n = 2 TRPC6$^{-/-}$ mice) wire to produce cohorts with statistically similar percent CCA dilation. Filled circles designate mice injured with an 0.014-inch wire. Open circles designate mice injured with an 0.018-inch wire. **B,** Representative hematoxylin and eosin staining of WT and TRPC6$^{-/-}$ uninjured and injured CCA 28 days after carotid wire injury. **C-F,** WT (n = 7 mice) and TRPC6$^{-/-}$ (n = 6 mice) mice were analyzed at 28 days after injury. Filled and open circles correspond to mice injured with 0.014-inch and 0.018-inch wires, respectively. **C,** Luminal area in uninjured and injured WT and TRPC6$^{-/-}$ mice at 28 days after carotid wire injury. **D,** Percent change in luminal area in injured WT and TRPC6$^{-/-}$ CCA after carotid wire injury. **E,** The percent change in the area inside the external elastic lamina (*EEL*). **F,** The percent change in medial thickness.

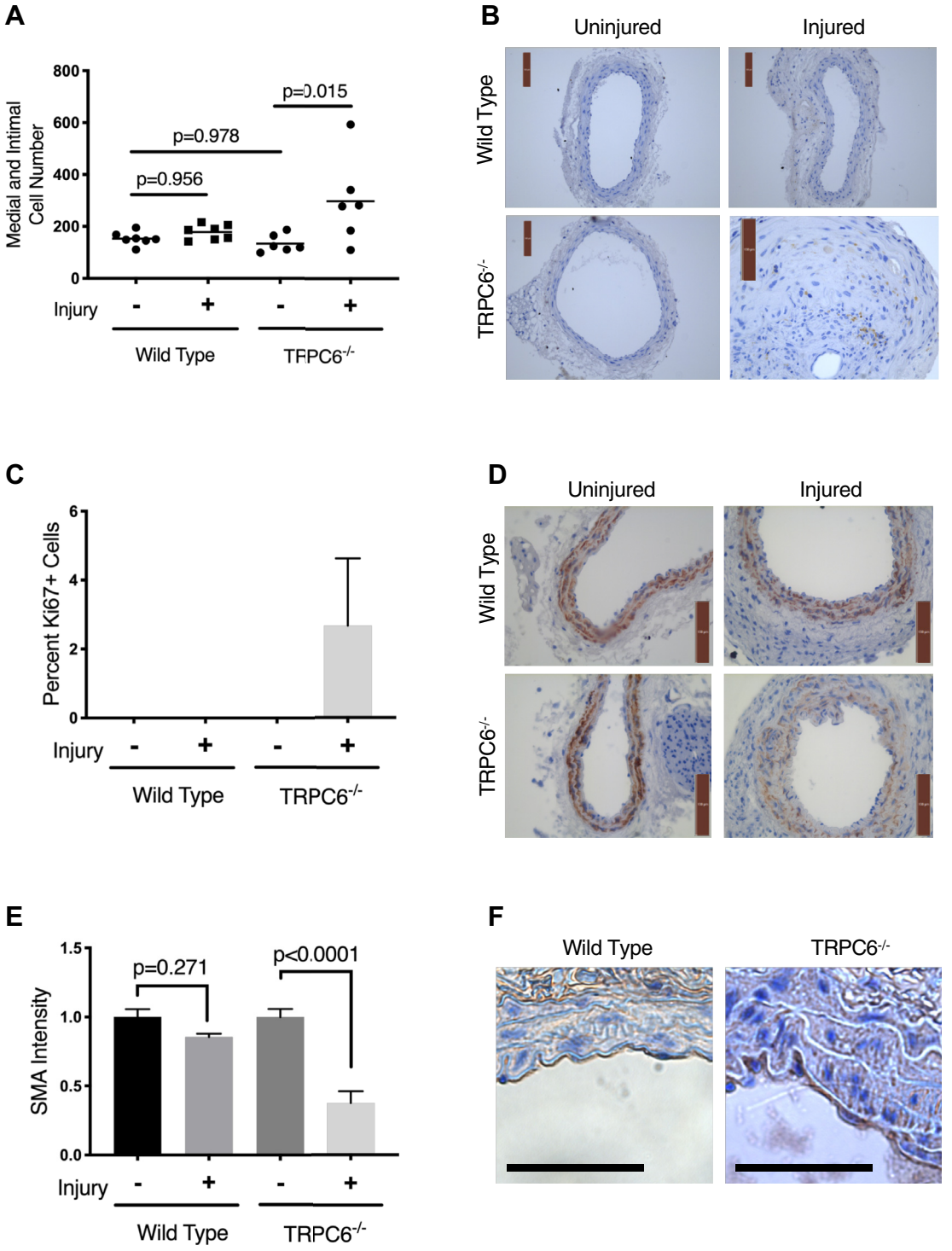

Fig 3. Cell proliferation and SMC dedifferentiation are accentuated in canonical transient receptor potential 6 deficient (*TRPC6*$^{-/-}$) mice after carotid wire injury. Wild-type (WT; n = 7 mice) and TRPC6$^{-/-}$ (n = 6 mice) mice were analyzed at 28 days after carotid wire injury. **A,** Medial and intimal cell nuclei were counted in uninjured and injured WT and TRPC6$^{-/-}$ CCA cross-sections. **B** and **C,** Active cell proliferation at 28 days after wire injury was assessed in uninjured and injured CCA cross-sections by Ki67 staining. **B,** Representative Ki67 staining. **C,** The percent of Ki67-positive cell nuclei was quantified and depicted in graphic form (n = 3 mice per genotype). **D** and **E,** Immunohistochemistry was performed for α-smooth muscle actin (α-*SMA*) on cross sections from injured and uninjured CCA from WT and TRPC6$^{-/-}$ mice. **D,** Representative α-SMA staining. **E,** Relative intensity of medial SMA staining was assessed semiquantitatively using Image J software on cross sections from uninjured and injured CCA from WT and TRPC6$^{-/-}$ mice and depicted graphically (n = 3 mice per genotype). **F,** Representative immunostaining for Von-Willebrand factor in injured WT and TRPC6$^{-/-}$ CCA at 100× objective. Scale bar (*black bar*) = 50 μm.

media of *TRPC6*$^{-/-}$ CCA after injury (a 62.4% decrease; n = 3 TRPC6$^{-/-}$ mice; $P < .0001$), suggesting that phenotypic modulation of TRPC6$^{-/-}$ VSMC was more extensive and/or more persistent in *TRPC6*$^{-/-}$ mice after vascular injury (Fig 3, *E*). Von-Willebrand factor staining for the detection of ECs was similar in injured WT and TRPC6$^{-/-}$ CCA. No significant Von-Willebrand factor staining was observed outside the endothelial monolayer (Fig 3, *F*).

To determine if baseline differences in SMC phenotype contributed to the aggressive luminal narrowing seen in some *TRPC6*$^{-/-}$ mice, SMC were harvested from WT and *TRPC6*$^{-/-}$ mice to study proliferation and migration. The 96-hour growth curves revealed that the relative cell number of *TRPC6*$^{-/-}$ cells increased to 7.2 ± 1.3 times that of the 24-hour cell number, whereas WT cells increased to 4.7 ± 0.6 times that of the 24-hour cell number (Fig 4, *A*; n = 5; $P = .001$). The fitted doubling time was 25.01 ± 2.35 hours for *TRPC6*$^{-/-}$ VSMC vs 34.39 ± 4.17 hours for WT VSMC. Growth studies in response to stimulation revealed a significant increase in the relative number of *TRPC6*$^{-/-}$ VSMC compared with WT VSMC in response to 10% FBS (2.7 ± 0.8 fold increase vs 1.8 ± 0.6 fold increase; n = 4; $P = .005$; Fig 4, *B*). No significant differences in cell number between WT and *TRPC6*$^{-/-}$ VSMC in response to PDGF-BB were identified. These data suggested that *TRPC6*$^{-/-}$ VSMC and WT VSMC differ in their potential to proliferate in culture with serum stimulation.

IH results from migration of a subset of clonally proliferative VSMC into the subendothelial space.[22] Therefore, in vitro migration of WT and *TRPC6*$^{-/-}$ VSMC was compared in scratch assays. At 12 hours after injury, wound closure was significantly enhanced in *TRPC6*$^{-/-}$ VSMC compared with WT VSMC in the presence of 10% FBS (64 ± 5% closure in *TRPC6*$^{-/-}$ VSMC vs 42 ± 6% closure in WT VSMC; n = 4; $P < .001$; Fig 4, *C*). The increased wound closure in *TRPC6*$^{-/-}$ VSMC incubated with 10 ng/mL PDGF-BB did not reach statistical significance (Fig 4, *D*). These data suggested that cell migration was increased in serum-stimulated *TRPC6*$^{-/-}$ VSMC compared with WT VSMC.

Enhanced proliferation and migration of *TRPC6*$^{-/-}$ VSMC in culture suggested that *TRPC6*$^{-/-}$ VSMC were phenotypically modulated to a more proliferative phenotype than WT VSMC. To explore this, the expression of contractile biomarkers was studied. Protein expression of MYH11 (a smooth muscle myosin) and SM22 (a smooth muscle actin binding protein) was significantly attenuated in *TRPC6*$^{-/-}$ VSMC (Fig 5, *A-C*). Compared with WT VSMC, MYH11 protein expression was reduced by 87.1 ± 10.6% ($P = .001$; n = 3; Fig 5 *A* and *B*) and SM22 protein expression was reduced by 83.7 ± 10.3% ($P = .001$; n = 3; Fig 5 *A* and *C*) in *TRPC6*$^{-/-}$ VSMC. Similarly, immunohistochemistry of CCA removed from WT and *TRPC6*$^{-/-}$ mice showed less staining for MYH11 and SM22 proteins in the media of *TRPC6*$^{-/-}$ CCA compared with WT CCA (Fig 5, *D*). A negative control using secondary antibody in the absence of primary antibody showed trace DAB staining outside the tunica media (Supplementary Fig). These data suggested that contractile biomarker proteins were decreased in the SMC of *TRPC6*$^{-/-}$ mice compared with WT mice.

To determine if differences in contractile biomarkers persisted with prolonged culture, SM22 expression was assessed through passage seven. As determined by immunoblot analysis, SM22 expression was 50.3% lower in *TRPC6*$^{-/-}$ VSMC compared with WT VSMC at passage one, 58.7% lower ($P = .0056$) at passage four, and 83.7% lower ($P = .0012$) at passage seven (Fig 5, *E*). No significant difference in the ratio of beta actin to GAPDH protein expression was found between WT and *TRPC6*$^{-/-}$ SMC, suggesting either beta actin or GAPDH were acceptable loading controls (Fig 5, *F* and *G*).

In addition to protein levels of MYH11 and SM22, mRNA levels were assessed by quantitative real-time PCR (Fig 5, *H* and *I*). Average mRNA level in WT was arbitrarily set as 1.0. MYH11 mRNA was significantly decreased in *TRPC6*$^{-/-}$ VSMC relative to WT VSMC (1 ± 0.25 in WT VSMC and 0.0031 ± 0.0023 in *TRPC6*$^{-/-}$ VSMC; n = 3; $P = .019$; Fig 5, *H*). SM22 mRNA was also significantly lower in *TRPC6*$^{-/-}$ VSMC relative to WT VSMC (1 ± 0.10 in WT and 0.20 ± 0.05 in *TRPC6*$^{-/-}$SMC; n = 4; $P = .0005$; Fig 5, *I*). WT and *TRPC6*$^{-/-}$ SMC GAPDH mRNA levels differed by less than one C_t in all experiments (data not shown). Thus, cultured *TRPC6*$^{-/-}$ VSMC were phenotypically modulated and had significantly lower levels of contractile biomarker mRNA and protein.

TRPC6$^{-/-}$ mice demonstrate compensatory upregulation of TRPC3 mRNA[13] and protein (Fig 6, *A*), so the effects of siRNA-mediated TRPC6 knockdown on contractile biomarker levels were assessed in MOVAS cells (ATCC CRL2797). MOVAS cells were transiently transfected with 50 nmol/L scrambled control (NsiRNA) or TRPC6 siRNA. Immunoblot analysis demonstrated 65.7% knockdown of TRPC6 protein 48 hours after the initiation of transfection (Fig 6, *B* and *C*). No differences were observed in the expression of TRPC3 at 48 hours in NsiRNA and TRPC6 siRNA transfected MOVAS cells (Fig 6, *B*). TRPC6-depleted MOVAS cells expressed significantly less MYH11 and SM22 protein than control transfected cells (52.8 ± 13.5% lower MYH11; n =3; $P = .017$; 49.6 ± 14.3% lower SM22; n =3; $P = .026$; Fig 6, *D-F*). These data suggested that acute knockdown of TRPC6 is sufficient to decrease contractile biomarkers in SMC.

DISCUSSION

We hypothesized that TRPC6 was essential in the maintenance or reexpression of a differentiated SMC phenotype and minimized luminal stenosis following arterial injury. Furthermore, we hypothesized that TRPC6$^{-/-}$ SMC demonstrated intrinsic differences in phenotype at baseline and in response to wire injury. Examination of carotid healing at 28 days after wire injury revealed increased

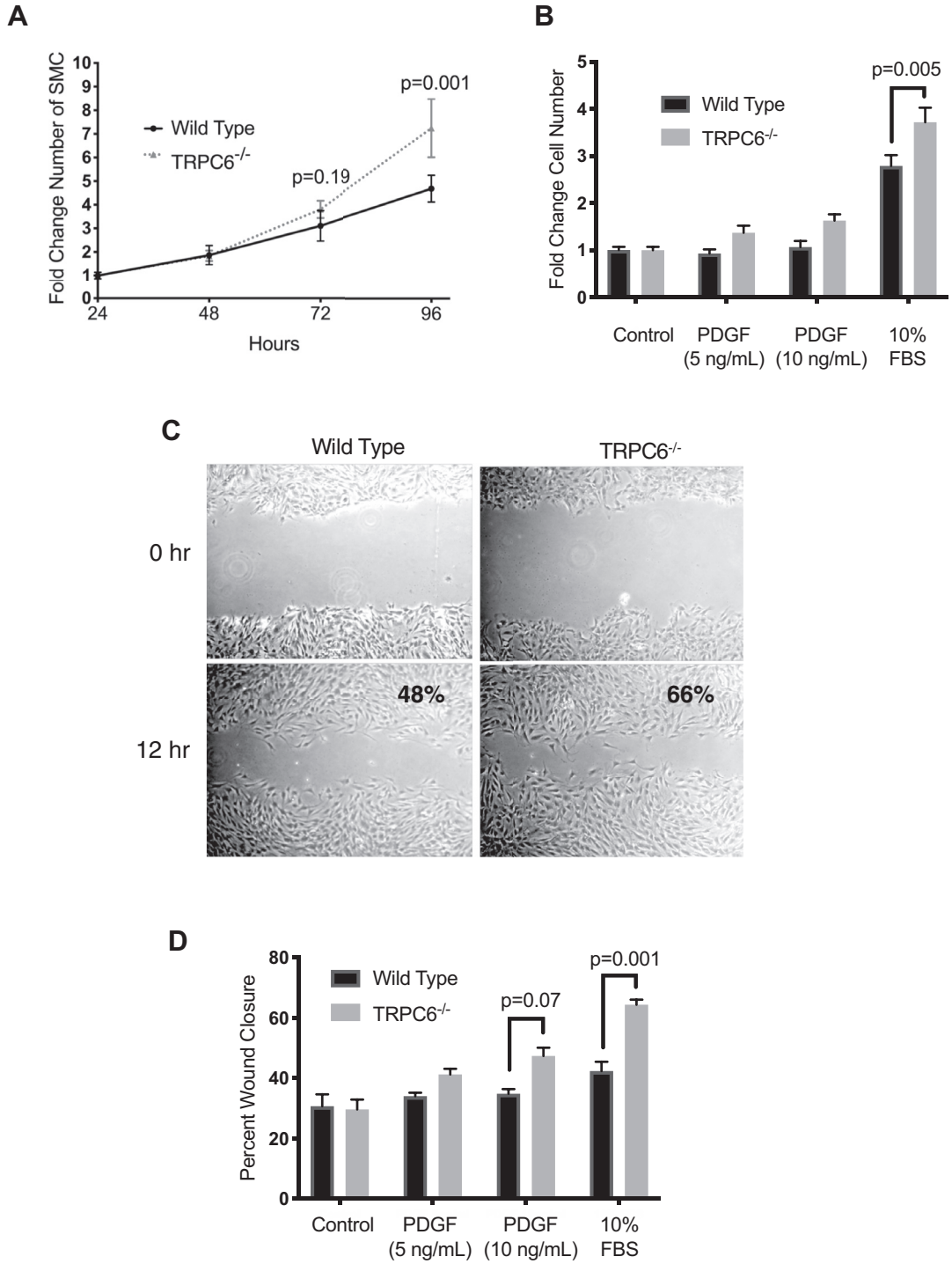

Fig 4. Increased proliferation and migration of cultured canonical transient receptor potential 6 deficient (*TRPC6*$^{-/-}$) mouse aortic smooth muscle cells (VSMC). **A**, WT and TRPC6$^{-/-}$ VSMC (passages 6-8) were incubated in culture media (DMEM + 20% fetal bovine serum [*FBS*]) for 24, 48, 72, and 96 hours. Cell number was determined at each time point. The increase in cell number relative to the number at 24 hours is depicted graphically. The increase in WT and TRPC6$^{-/-}$ VSMC were compared by Student's t test at 72 and 96 hours (n = 5) **(B)** WT and TRPC6$^{-/-}$ VSMC were serum starved overnight and incubated with control medium (0.25% FBS), 5 ng/mL platelet-derived growth factor (*PDGF*)-BB, 10 ng/mL PDGF-BB, or 10% FBS for 48 hours. The increase in cell number relative to control was determined at 48 hours (n = 4). **C** and **D**, WT and TRPC6$^{-/-}$ VSMC (passages 6-8) were serum starved overnight and subjected to scrape assays. Scraped cells were immediately washed and incubated with control medium (0.25% FBS), 5 ng/mL PDGF-BB, 10 ng/mL PDGF-BB, or 10% FBS. The wound area was determined at 0 and 12 hours after scaping and percent wound closure at 12 hours was calculated. **C**, Representative scrape assay after 10% FBS stimulation; percent wound closure at 12 hours is listed in the lower panels. **D**, Graphic representation of percent wound closure (n = 4).

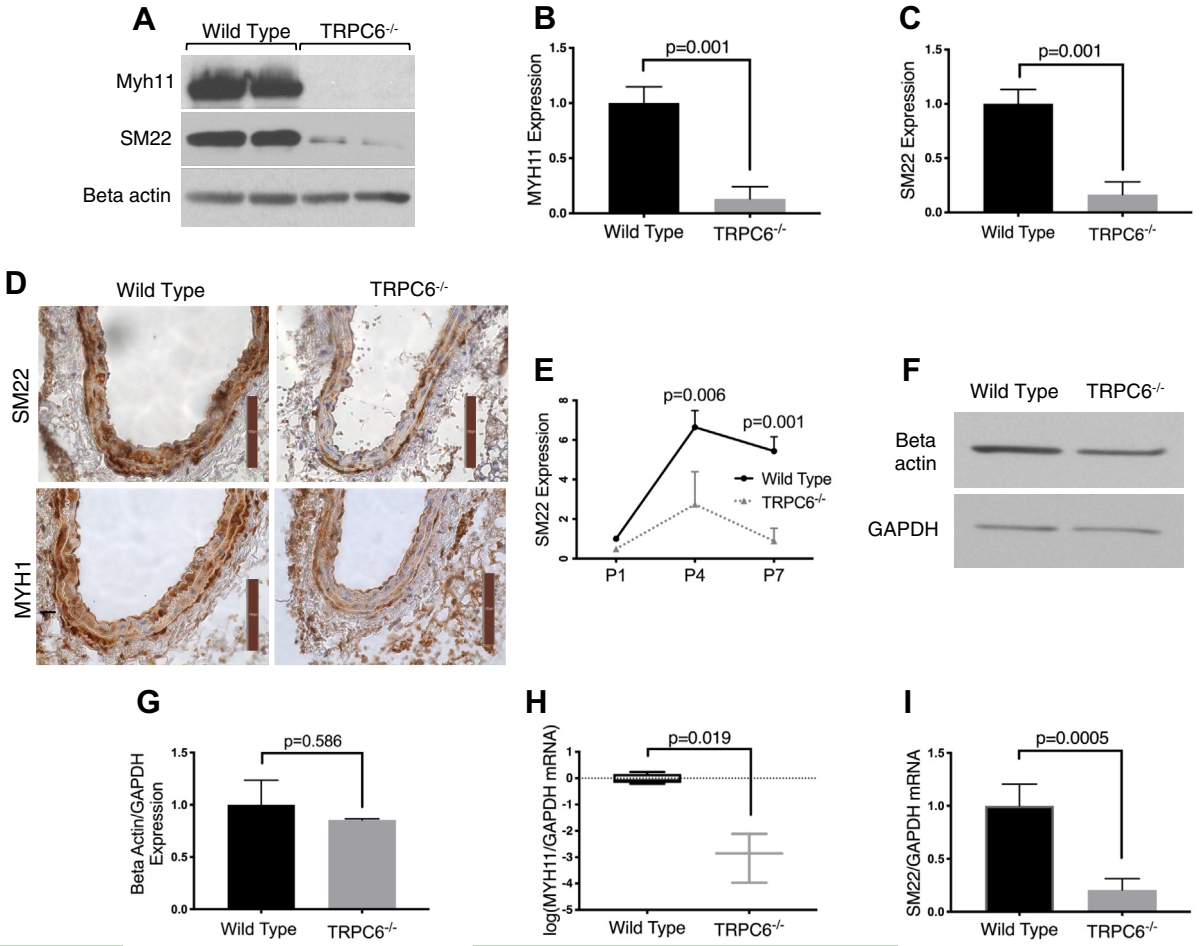

Fig 5. Canonical transient receptor potential 6 deficient (*TRPC6*$^{-/-}$) SMC are phenotypically modulated in culture and in situ. **A-C**, Lysates were prepared from cultured wild-type (WT) and TRPC6$^{-/-}$ VSMC (passages 6-8), resolved by sodium dodecyl sulfate polyacrylamide gel electrophoresis, and immunoblotted for SM22 and MYH11. Actin served as the loading control. **A**, Representative immunoblot. **B** and **C**, Relative MYH11 and SM22 protein expression quantified by densitometry (n = 3 immunoblots). **D**, Immunohistochemistry (IHC) performed on common carotid artery (CCA) cross-sections of 8- to 10-week-old male WT and TRPC6$^{-/-}$ mice. (*Top*) IHC for SM22 and (*Bottom*) MYH11. **E**, SM22 protein levels were assessed at passages 1, 4, and 7 in WT and TRPC6$^{-/-}$ VSMC by immunoblot analysis and quantified by densitometry. **F** and **G**, Lysates were prepared from cultured WT and TRPC6$^{-/-}$ VSMC (passages 6-8) and immunoblotted for beta-actin and GAPDH. **F**, Representative western blot. **G**, The ratio of beta actin to GAPDH protein was quantified by densitometry (n = 3). **H** and **I**, Relative MYH11 and SM22 mRNA levels were assessed by quantitative real-time PCR in cultured WT and TRPC6$^{-/-}$ VSMC (passages 6-8; n = 4).

SMC proliferation and luminal narrowing in *TRPC6*$^{-/-}$ mice compared with WT mice. No differences in re-endothelialization were observed between WT and TRPC6$^{-/-}$ mice at 28 days, which is consistent with our previous results showing normal rates of endothelial migration in chow-fed TRPC6$^{-/-}$ mice. Immunohistochemistry suggested decreased expression of biomarkers of the contractile phenotype, MYH11 and SM22, in the uninjured CCA of *TRPC6*$^{-/-}$ mice compared with WT mice. Additional in vitro studies showed that arterial SMC of *TRPC6*$^{-/-}$ mice are phenotypically modulated compared with WT SMC, with reduced levels of MYH11 and SM22 in*TRPC6*$^{-/-}$ SMC. Differences in contractile biomarkers persisted or increased through serial passages in culture. Moreover, acute downregulation of *TRPC6* using siRNA resulted in decreased expression of SM22 and MYH11 in immortalized mouse aortic SMC, suggesting that TRPC6 was important for the expression of contractile biomarkers. In total, these findings suggest that TRPC6 contributes to VSMC phenotypic regulation. Although our data also suggests that loss of TRPC6 promotes SMC proliferation in vitro and after carotid wire injury, we cannot discount the possibility that TRPC6 regulates SMC apoptosis to increase cell viability.

Our in vivo studies show distinct differences between the CCA of WT and *TRPC6*$^{-/-}$ mice, including increased

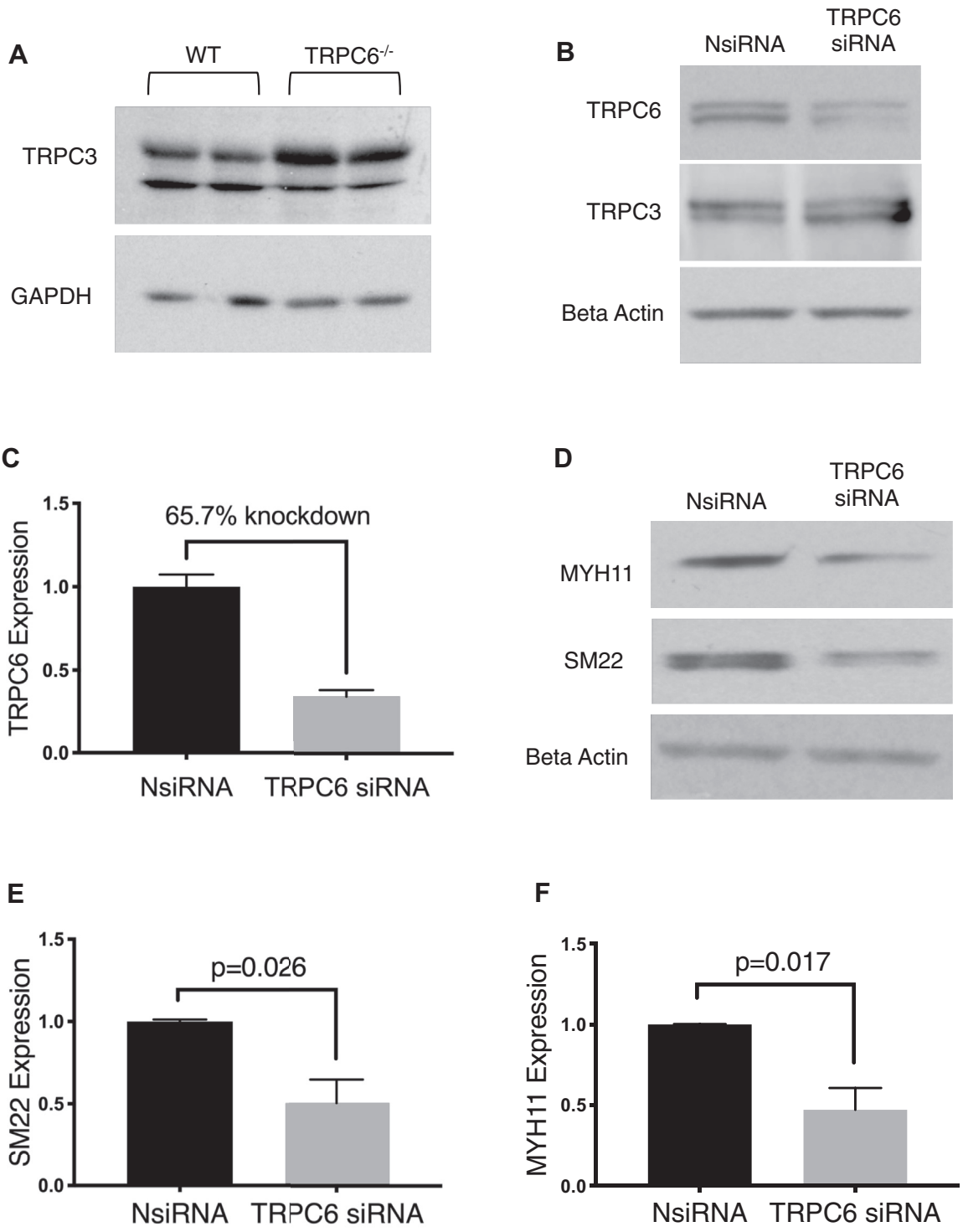

Fig 6. Acute, transient knockdown of canonical transient receptor potential 6 (TRPC6) promotes loss of the contractile phenotype in MOVAS cells. **A**, Wild-type (*WT*) and TRPC6$^{-/-}$ CCA from 10-week-old male mice were explanted and homogenized in lysis buffer (n = 3 mice and 6 CCA per genotype). Lysates were resolved by SDS page and immunoblotted against TRPC3 and GAPDH. **B-F**, Immortalized mouse aortic smooth muscle cell line (MOVAS) cells were transiently transfected with 50 nmol/L control small interfering RNA (*NsiRNA*) or TRPC6 siRNA. Transfected cells were harvested at 48 hours and immunoblotted for TRPC6, TRPC3, and contractile biomarkers. **B**, Representative immunoblot of total TRPC6 and TRPC3 protein. **C**, Relative TRPC6 protein expression in NsiRNA and TRPC6 siRNA transfected cells was quantified by densitometry (n = 3). **D**, Representative immunoblot of contractile biomarkers. **E** and **F**, Relative protein expression of MYH11 and SM22 in NsiRNA and TRPC6 siRNA transfected cells quantified by densitometry (n = 3).

luminal area, decreased wall thickness, and decreased elastic lamellae in *TRPC6*$^{-/-}$ CCA. Therefore, in our injury model, wire size was selected to obtain a similar degree of dilation in WT and TRPC6$^{-/-}$ carotid arteries. Within the limited range of dilation that resulted, there was no correlation between the degree of carotid dilation during wire injury and injury severity at 28 days. Similarly, we did not observe an association between the wire size employed in our injury model (0.014- and 0.018-inch) and injury severity. The altered, uninjured carotid artery structure of TRPC6$^{-/-}$ mice is potentially explained by diminished expression of contractile biomarkers. Decreased postnatal expression of contractile biomarkers in situ is associated with structural deficits and dilation of systemic arteries.[23] The larger carotid arteries of *TRPC6*$^{-/-}$ mice also suggest that basal smooth muscle tone is decreased. This is in contrast with contraction in response to an agonist that is increased in *TRPC6*$^{-/-}$ aortic and cerebral arterial SMC.[13] Increased agonist-induced contraction is attributed to SMC overexpression of TRPC3 in these studies.[13] TRPC3 is overexpressed in the CCA of *TRPC6*$^{-/-}$ mice compared with WT mice (Fig 6, *A*); however, the role of TRPC3 overexpression in basal tone and contractile biomarker expression in the CCA is unclear. Because acute downregulation of TRPC6 in vitro using siRNA is accompanied by a decrease in SM22 and MYH11, the reduction of TRPC6, and not the upregulation of TRPC3, seems to be responsible for the decrease in contractile biomarkers seen in the *TRPC6*$^{-/-}$ mice.

Calcium channels are important in many aspects of SMC function, including phenotype regulation. Calcium influx through voltage-gated channels can induce the expression of SMC differentiation marker genes.[24] TRPC6, a non-voltage-gated channel, promotes contractile gene expression in differentiating myofibroblasts after injury,[25] and TRPC6 is required for transforming growth factor-β1-induced α-SMA expression in murine cardiac, intestinal, and pulmonary myofibroblasts.[25-27] Our findings suggest that TRPC6 also supports the expression of contractile biomarkers in arterial SMC. It is interesting to speculate that TRPC6 may modulate the expression or activity of calcium-dependent master transcription factors involved in the epigenetic regulation of SMC phenotype. The transcription factors MEF2C and myocardin are known to be regulated by the calcium/calmodulin-kinase and calcineurin axis as well as RhoA/ROCK kinases, all of which have been shown to be potently induced by TRPC6 activation.[28-30] Altered master transcription factor activity and epigenetic changes may facilitate phenotypic modulation, downregulation of contractile biomarkers, and dysregulated elastin synthesis in TRPC6-deficient SMC.[7]

The role of TRPC6 in the expression of contractile biomarkers may vary between the basal state and agonist-induced differentiation. A recent study by Numaga-Tomita et al[31] shows that transforming growth factor-β1-stimulated contractile differentiation and expression of SM22 is enhanced in aortic SMC harvested from *TRPC6*$^{-/-}$ mice compared with WT mice. No difference is seen in the basal expression of SM22 between serum-starved WT and *TRPC6*$^{-/-}$ aortic SMC, which contrasts with our findings with SMC grown in serum-supplemented medium. Differences in age (5 vs 10 weeks) and strain of mice used for SMC harvest, or serum exposure, could explain the discrepant findings. In addition, serum composition and cell confluency can influence SMC phenotype and contractile gene expression.[32-34] The variability of primary SMC in culture underscores the importance of in vivo studies to assess the relevance of in vitro findings.

The function of TRPC6 in SMC proliferation and phenotypic modulation varies with the vascular bed from which the SMC are harvested. PDGF stimulates pulmonary artery SMC proliferation by upregulating TRPC6, and the action of PDGF is decreased by TRPC6 downregulation.[35] In contrast, TRPC6 deficiency does not alter the proliferative response of aortic SMC to PDGF-BB in our studies or those of Numaga-Tomita et al.[31] Dissimilarities in the role of TRPC6 in proliferation of pulmonary artery SMC and systemic arterial SMC may be a reflection of the regional heterogeneity of SMC. Because SMC from various tissue beds differ in embryonic origin and in function, it is not surprising that the role of TRPC6 varies as well.

The specific function of the increased TRPC6 in the response to arterial injury is unclear. To date, there are limited data on the expression patterns and activity of TRPC6 in human arterial intimal hyperplasia and restenosis after vascular intervention. The expression of TRPC6 in human restenotic lesions has not been assessed directly. Vascular TRPC6 mRNA has been found to increase after ex vivo balloon angioplasty of human internal mammary artery segments.[36] Balloon angioplasty acutely increases expression of TRPC6 in rat carotid arteries.[37] However, the functional relevance of altered TRPC6 expression after arterial angioplasty and the role it may play in the pathogenesis of intimal hyperplasia has not been investigated. Our finding that intimal hyperplasia and luminal stenosis are increased in TRPC6-deficient mice after carotid wire injury, suggests that TRPC6 might have a protective, homeostatic role. TRPC6 could be upregulated acutely after angioplasty to control the degree of SMC phenotype modulation to promote healing with preservation of the arterial lumen. Further studies are needed to explore this hypothesis.

Limitations of our studies include the use of a noninducible, global TRPC6 knockout mouse. We therefore cannot discount the contributions of TRPC6-deficient ECs, inflammatory cells, and fibroblasts to the cellularity of the CCA and the development of intimal hyperplasia after carotid arterial injury. Interaction between TRPC6

and PECAM1 in ECs, for example, is necessary for transendothelial migration of leukocytes into tissue.[38] Altered leukocyte diapedesis and local production of inflammatory mediators may modulate the SMC response to carotid wire injury in TRPC6$^{-/-}$ mice. TRPC6 has also been shown to mediate the effects of thromboxane receptor activation on platelet aggregation.[39] Decreased megakaryocyte and platelet TRPC6 may blunt platelet aggregation on denuded subendothelial collagen after wire injury, potentially contributing to abnormal arterial healing. Our study does not use littermate controls, although mouse lines were periodically backcrossed to minimize genetic drift. Although this study focuses on changes in expression of contractile biomarkers, it does not investigate the effects of TRPC6 depletion on SMC contractility. Regional heterogeneity in arterial SMC could potentially lead to inconsistencies between our in vivo (common carotid SMC) and in vitro (thoracic aortic SMC) model systems. The specific roles of TRPC6-mediated calcium flux and downstream signaling intermediates also remain undefined.

In conclusion, our study demonstrates that the contractile phenotype of VSMC is attenuated in *TRPC6*$^{-/-}$ mice. *TRPC6*$^{-/-}$ VSMC show increased proliferation and migration as well as decreased contractile biomarker expression. After carotid injury, *TRPC6*$^{-/-}$ mice display luminal narrowing and IH, with a significant increase in total cell number, active proliferation, and a loss of contractile biomarkers. Future mechanistic studies of VSMC phenotype modulation may suggest novel therapies for the management of intimal hyperplasia that target VSMC dedifferentiation without adversely affecting endothelial healing.

AUTHOR CONTRIBUTIONS

Conception and design: AS, PC, MR, LG
Analysis and interpretation: AS, PC, MR, LG
Data collection: AS, PP, ED, PC
Writing the article: AS, LG
Critical revision of the article: AS, PP, PC, LB, MR, LG
Final approval of the article: AS, PP, ED, PC, LB, MR, LG
Statistical analysis: AS
Obtained funding: LG
Overall responsibility: LG

REFERENCES

1. Fishman JA, Ryan GB, Karnovsky MJ. Endothelial regeneration in the rat carotid artery and the significance of endothelial denudation in the pathogenesis of myointimal thickening. Lab Invest 1975;32:339-51.
2. Haudenschild CC, Schwartz SM. Endothelial regeneration. II. Restitution of endothelial continuity. Lab Invest 1979;41:407-18.
3. Libby P, Schwartz D, Brogi E, Tanaka H, Clinton SK. A cascade model for restenosis: a special case of atherosclerosis progression. Circulation 1992;86(Suppl):47-52.
4. Goel SA, Guo LW, Liu B, Kent KC. Mechanisms of post-intervention arterial remodelling. Cardiovasc Res 2012;96:363-71.
5. Ghosh D, Syed AU, Prada MP, Nystoriak MA, Santana LF, Nieves-Cintron M, et al. Calcium channels in vascular smooth muscle. Adv Pharmacol 2017;78:49-87.
6. Owens GK. Regulation of differentiation of vascular smooth muscle cells. Physiol Rev 1995;75:487-517.
7. Gomez D, Swiatlowska P, Owens GK. Epigenetic control of smooth muscle cell identity and lineage memory. Arterioscler Thromb Vasc Biol 2015;35:2508-16.
8. Beech DJ. Ion channel switching and activation in smooth-muscle cells of occlusive vascular diseases. Biochem Soc Trans 2007;35:890-4.
9. Tang Q, Guo W, Zheng L, Wu JX, Liu M, Zhou X, et al. Structure of the receptor-activated human TRPC6 and TRPC3 ion channels. Cell Res 2018;28:746-55.
10. Dietrich A, Mederos y Schnitzler M, Kalwa H, Storch U, Gudermann T. Functional characterization and physiological relevance of the TRPC3/6/7 subfamily of cation channels. Naunyn Schmiedebergs Arch Pharmacol 2005;371:257-65.
11. Chaudhuri P, Colles SM, Bhat M, Van Wagoner DR, Birnbaumer L, Graham LM. Elucidation of a TRPC6-TRPC5 channel cascade that restricts endothelial cell movement. Mol Biol Cell 2008;19:3203-11.
12. Rosenbaum MA, Chaudhuri P, Graham LM. Hypercholesterolemia inhibits reendothelialization of arterial injuries by TRPC channel activation. J Vasc Surg 2015;62:1040-7.
13. Dietrich A, Mederos y Schnitzler M, Gollasch M, Gross V, Storch U, Dubrovska G, et al. Increased vascular smooth muscle contractility in *TRPC6*$^{-/-}$ mice. Mol Cell Biol 2005;25:6980-9.
14. Varghese F, Bukhari AB, Malhotra R, De A. IHC Profiler: an open source plugin for the quantitative evaluation and automated scoring of immunohistochemistry images of human tissue samples. PLoS One 2014;9:e96801.
15. Lindner V, Fingerle J, Reidy MA. Mouse model of arterial injury. Circ Res 1993;73:792-6.
16. Adhikari N, Shekar KC, Staggs R, Win Z, Steucke K, Lin YW, et al. Guidelines for the isolation and characterization of murine vascular smooth muscle cells. A report from the International Society of Cardiovascular Translational Research. J Cardiovasc Transl Res 2015;8:158-63.
17. Cory G. Scratch-wound assay. Methods Mol Biol 2011;769:25-30.
18. Chaudhuri P, Rosenbaum MA, Sinharoy P, Damron DS, Birnbaumer L, Graham LM. Membrane translocation of TRPC6 channels and endothelial migration are regulated by calmodulin and PI3 kinase activation. Proc Natl Acad Sci U S A 2016;113:2110-5.
19. Chaudhuri P, Rosenbaum MA, Birnbaumer L, Graham LM. Integration of TRPC6 and NADPH oxidase activation in lysophosphatidylcholine-induced TRPC5 externalization. Am J Physiol Cell Physiol 2017;313:C541-55.
20. Schmittgen TD, Livak KJ. Analyzing real-time PCR data by the comparative C(T) method. Nat Protoc 2008;3:1101-8.
21. Chalmers JA, Martino TA, Tata N, Ralph MR, Sole MJ, Belsham DD. Vascular circadian rhythms in a mouse vascular smooth muscle cell line (Movas-1). Am J Physiol Regul Integr Comp Physiol 2008;295:R1529-38.
22. Shi N, Chen SY. Smooth muscle cell differentiation: model systems, regulatory mechanisms, and vascular diseases. J Cell Physiol 2016;231:777-87.
23. Huang J, Wang T, Wright AC, Yang J, Zhou S, Li L, et al. Myocardin is required for maintenance of vascular and visceral smooth muscle homeostasis during postnatal development. Proc Natl Acad Sci U S A 2015;112:4447-52.
24. Wamhoff BR, Bowles DK, McDonald OG, Sinha S, Somlyo AP, Somlyo AV, et al. L-type voltage-gated Ca2+ channels modulate expression of smooth muscle differentiation marker genes via a rho kinase/myocardin/SRF-dependent mechanism. Circ Res 2004;95:406-14.

25. Davis J, Burr AR, Davis GF, Birnbaumer L, Molkentin JD. A TRPC6-dependent pathway for myofibroblast transdifferentiation and wound healing in vivo. Dev Cell 2012;23:705-15.
26. Kurahara LH, Sumiyoshi M, Aoyagi K, Hiraishi K, Nakajima K, Nakagawa M, et al. Intestinal myofibroblast TRPC6 channel may contribute to stenotic fibrosis in Crohn's disease. Inflamm Bowel Dis 2015;21:496-506.
27. Hofmann K, Fiedler S, Vierkotten S, Weber J, Klee S, Jia J, et al. Classical transient receptor potential 6 (TRPC6) channels support myofibroblast differentiation and development of experimental pulmonary fibrosis. Biochim Biophys Acta Mol Basis Dis 2017;1863:560-8.
28. Singer HA. Ca2+/calmodulin-dependent protein kinase II function in vascular remodelling. J Physiol 2012;590:1349-56.
29. Ginnan R, Sun LY, Schwarz JJ, Singer HA. MEF2 is regulated by CaMKIIdelta2 and a HDAC4-HDAC5 heterodimer in vascular smooth muscle cells. Biochem J 2012;444:105-14.
30. Pagiatakis C, Gordon JW, Ehyai S, McDermott JC. A novel RhoA/ROCK-CPI-17-MEF2C signaling pathway regulates vascular smooth muscle cell gene expression. J Biol Chem 2012;287:8361-70.
31. Numaga-Tomita T, Shimauchi T, Oda S, Tanaka T, Nishiyama K, Nishimura A, et al. TRPC6 regulates phenotypic switching of vascular smooth muscle cells through plasma membrane potential-dependent coupling with PTEN. FASEB J 2019;33:9785-96.
32. Erac Y, Selli C, Kosova B, Akcali KC, Tosun M. Expression levels of TRPC1 and TRPC6 ion channels are reciprocally altered in aging rat aorta: implications for age-related vasospastic disorders. Age (Dordr) 2010;32:223-30.
33. Fager G, Hansson GK, Gown AM, Larson DM, Skalli O, Bondjers G. Human arterial smooth muscle cells in culture: inverse relationship between proliferation and expression of contractile proteins. Vitro Cell Dev Biol 1989;25:511-20.
34. Pauly RR, Passaniti A, Crow M, Kinsella JL, Papadopoulos N, Monticone R, et al. Experimental models that mimic the differentiation and dedifferentiation of vascular cells. Circulation 1992;86(Suppl):68-73.
35. Yu Y, Sweeney M, Zhang S, Platoshyn O, Landsberg J, Rothman A, et al. PDGF stimulates pulmonary vascular smooth muscle cell proliferation by upregulating TRPC6 expression. Am J Physiol Cell Physiol 2003;284:C316-30.
36. Bergdahl A, Gomez MF, Wihlborg AK, Erlinge D, Eyjolfson A, Xu SZ, et al. Plasticity of TRPC expression in arterial smooth muscle: correlation with store-operated Ca2+ entry. Am J Physiol Cell Physiol 2005;288:C872-80.
37. Jia S, Rodriguez M, Williams AG, Yuan JP. Homer binds to Orai1 and TRPC channels in the neointima and regulates vascular smooth muscle cell migration and proliferation. Sci Rep 2017;7:5075.
38. Weber EW, Han F, Tauseef M, Birnbaumer L, Mehta D, Muller WA. TRPC6 is the endothelial calcium channel that regulates leukocyte transendothelial migration during the inflammatory response. J Exp Med 2015;212:1883-99.
39. Vemana HP, Karim ZA, Conlon C, Khasawneh FT. A critical role for the transient receptor potential channel type 6 in human platelet activation. PLoS One 2015;10:e0125764.

Submitted Mar 31, 2020; accepted Jul 6, 2020.

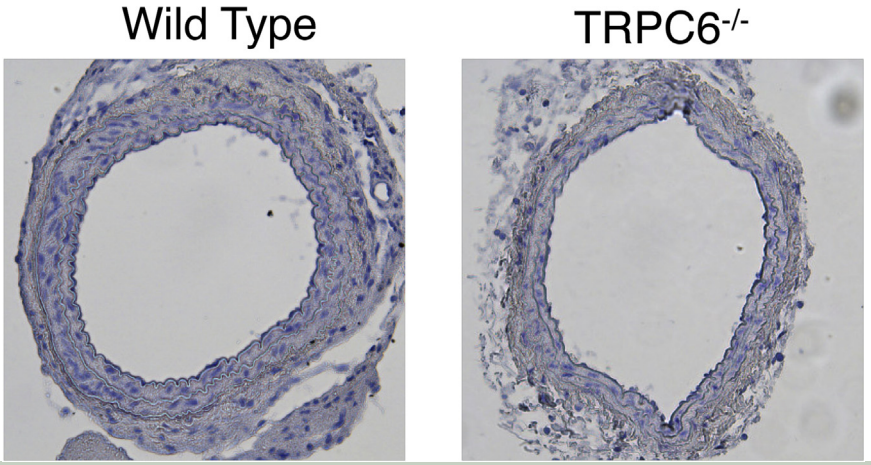

Supplementary Fig. As a negative control, immunohistochemistry was performed against uninjured wild-type (WT) and canonical transient receptor potential 6 deficient (*TRPC6*$^{-/-}$) CCA cross-sections in the absence of a primary antibody. After overnight incubation in Tris-buffered saline (TBS) + 5% bovine serum albumin (BSA), sections were treated with goat, anti-rabbit secondary antibody (Invitrogen; cat. 31460, 1:1500) in TBS + 5% BSA for 2 hours. Sections were then developed with 3,3'diaminobenzidine (DAB).